An innovative multi-gap clutch based on magneto-rheological fluids and electrodynamic effects: magnetic design and experimental characterization

OPEN ACCESS
IOP Publishing
Smart Materials and Structures
Smart Mater. Struct. **26** (2017) 015007 (11pp)
doi:10.1088/0964-1726/26/1/015007

An innovative multi-gap clutch based on magneto-rheological fluids and electrodynamic effects: magnetic design and experimental characterization

R Rizzo

Department of Energy and Systems Engineering, University of Pisa, Largo Lucio Lazzarino, I-56122, Pisa, Italy

E-mail: rocco.rizzo@unipi.it

Received 22 September 2016, revised 5 November 2016
Accepted for publication 14 November 2016
Published 5 December 2016

Abstract

In this paper an innovative multi-gap magnetorheological clutch is described. It is inspired by a device previously developed by the author's research group and contains a novel solution based on electrodynamic effects, capable to considerably improve the transmissible torque during the engagement phase. Since this (transient) phase is characterized by a non-zero angular speed between the two clutch shafts, the rotation of a permanent magnets system, used to excite the fluid, induces eddy currents on some conductive material strategically positioned in the device. As a consequence, an electromagnetic torque is produced which is added to the torque transmitted by the magnetorheological fluid only. Once the clutch is completely engaged and the relative speed between the two shafts is zero, the electrodynamic effects vanish and the device operates like a conventional magnetorheological clutch. The system is investigated and designed by means a 3D FEM model and the performance of the device is experimentally validated on a prototype.

Keywords: magneto-rheological fluid, eddy currents, electromagnetic torque, magneto-rheological clutch

(Some figures may appear in colour only in the online journal)

1. Introduction

In a recent paper [1] the author's research group presented and discussed a fail-safe, multi-gap magnetorheological clutch, excited by means of a system of permanent magnets. It was developed in a framework of a project aimed to reduce the energy consumption of the vacuum pump in a servo assisted brake system for automotive applications [2, 3]. The clutch was interposed between the cam shaft and the vacuum pump in order to disengage the pump when its operation is no longer necessary.

The choice of a magnetorheological (MR) fluid-based clutch, powered by permanent magnets, was suggested by several design constraints [4, 5]. In particular, the safety requirements of the braking system needed the clutch to be fail-safe, and no axial load had to be exerted on the cam-shaft. Then, since the magnetorheological fluid (MRF) used to built the clutch is characterized by low viscosity when unmagnetized (<0.3 Pa s), low power losses in the disengaged condition was assured. Furthermore it was able to produce high transmissible torque in the engaged condition due to high yield stress when magnetized ($\simeq 70$ kPa, @200 kA m^{-1}). Finally, since the MRF responds in a fast switching time (<10 to 12 ms) when it passes from unmagnetized to

magnetized state (and vice versa), the clutch actuation was within the time-response requirements. The device developed in [1] was investigated and designed by means a proper 3D FEM model. Furthermore it was experimentally characterized by performing a set of measurements on a dedicated test bench. As described in [6], that MRF-based clutch allowed to reduce the consumption of the vacuum pump up to 29% in urban driving and 46% in extra-urban driving.

Although the developed prototype [1] operates quite well [7], its main drawback is the value of the transmissible torque in the starting phase, that is during the mechanical transient between the disengaged and the engaged condition. A shown in figure 3(b), the torque in the engaged condition is almost constant as a function of the relative speed ($\Delta\Omega$) between the two clutch shafts. This is due to the fact that, in the engaged condition, the torque component related to the viscosity, which depends on $\Delta\Omega$, is about 6% of the magnetic-field-dependent torque component.

In this new paper, an innovative configuration is presented capable to overcome the main drawback of the previously developed prototype. The new device exploits the electrodynamic effects produced by a rotating magnetic field to considerably improve the performance of the clutch. During the engagement (transient) phase, the rotation of the excitation system composed of permanent magnets induces 'eddy currents' on a conductive material, strategically positioned in the device. Then, the interaction between these currents and the excitation magnetic field produces an electromagnetic torque. This torque is added to the one transmitted by the fluid only, helping the clutch engagement, especially during the starting phase when extra torque could be necessary to overcome possible static frictions. However, once the two shafts have reached the same speed, the eddy currents (and consequently the electromagnetic torque) vanish and the torque transmission is assured by the MRF only, as in conventional MRF-based clutch.

The paper is organized as follows. Section 2 briefly describes the previously developed device and its operation; section 3 presents the new proposed device; section 4 synthesizes the electro-dynamic FEM model with the simulations results; section 5 describes the prototype and discusses the experimental results, measured using a suitable test bench.

2. The previously developed prototype: brief description

For the sake of subsequent clarity and in order to introduce the new configuration, the previously developed device (hereafter referred to as 'old device') and its operation were briefly synthesized. Anyhow, a detailed description is reported in [1, 8]. As shown in figure 1 it was composed of a primary and a secondary shaft, of a a double cup-shaped gap, filled with MRF, and of a permanent magnets excitation system (PMs), which can slide axially in the housing chamber. The AISI-1018 and AISI-316L materials were used for the ferromagnetic and non-ferromagnetic parts respectively; while the MRF140CG, produced by Lord Corporation [9], was chosen as the MRF. Concerning the magnetic field source, the highest MRF excitation level was obtained by using a rare Earth NdFeB hollow cylinder, arranged in four 90°-poles, and alternately magnetized along their diametral direction, as shown in figure 2.

The device operates as follows: when the PM is far from the MRF gap (figure 1(a), 'OFF state'), a very low magnetic flux density passes through the fluid. In this condition the transmitted torque, mainly due to parasitic and residual magnetization effects, has a very low value ($\simeq$0.4 to 0.5 N m), resulting in a condition of disengaged shafts. On the contrary, during the PM movement from the OFF to the ON state, as the distance between the magnets and the fluid is reducing, the magnetic field inside the MRF increases. Then, when the PMs system is in the 'ON state' (figure 1(b)), the magnetic flux density is high enough to result in a high shear-stress and consequently in a high level of transmissible torque ($\simeq$5.0 N m) between the primary and secondary shaft. However, besides the transmissible torque, also a magnetic axial force should be considered in the design phase. This force is due to the natural attractive behavior between PMs and ferromagnetic materials. Since it acts in the axial direction, it may either hinders or facilitates the PM motion from the OFF state to the ON state and vice versa. Figure 3(a) shows the transmissible torque and the magnetic axial force as a function of the excitation system displacement from the OFF to the ON state. Figure 3(b) shows the profile of the transmissible torque (in the OFF and ON state) as a function of the relative speed $\Delta\Omega$ between the primary and secondary shaft.

As for the clutch actuation (not shown in the figures) a system based on a passive pneumatic operating principle was recognized as the most suitable for the specific application. A solution, which proved to be effective and reliable in the on/off control strategy, is described in details in [2, 10]. The magnet, by means of an o-ring seal, splits the chamber in two hermetically separated parts. The primary and secondary shafts present an axial hole, which connects each part of the magnet chamber with an external pressure source. The operation principle of this solution is as follows: the engagement phase (moving the PM from the OFF to the ON state position) is assured by a preloaded spring; the disengagement phase can be obtained by the different pressures acting on the opposite magnet surfaces, which determines the shift of the PM system back to the OFF position. Anyhow, the actuation system was designed so that the spring forces the magnet toward the fluid gap zone; this condition guarantees the fluid magnetization in case of pneumatic system failure, assuring a fail-safe clutch operation.

3. The *new* device

In the previous device, the primary shaft was composed of alternated ferromagnetic and non-ferromagnetic discs (see figure 4). As described in [1], this configuration was designed to force the magnetic flux density B to pass through the inner

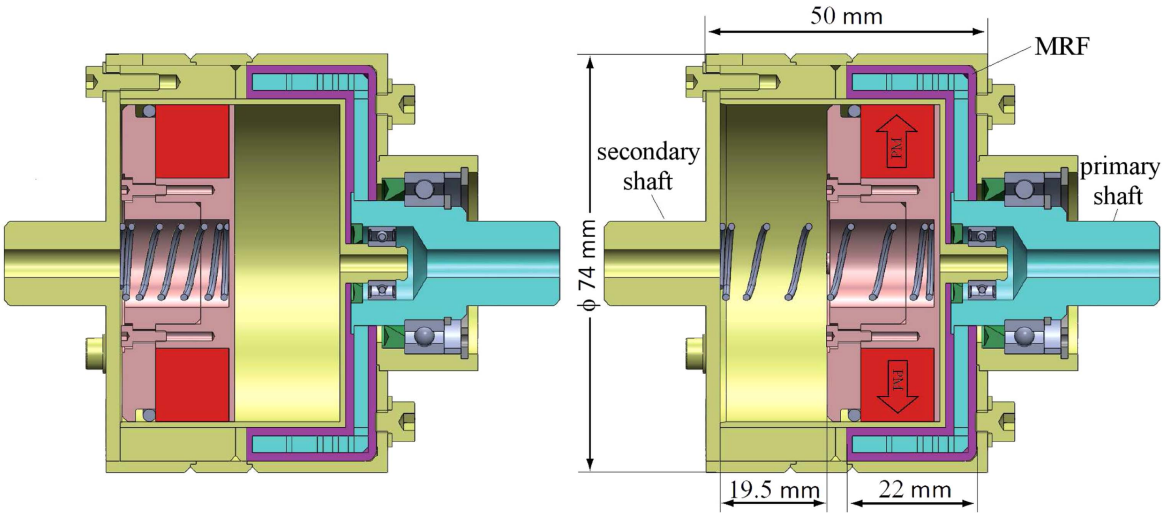

(a) Disengaged clutch (OFF state) (b) Engaged clutch (ON state)

Figure 1. Previous clutch prototype scheme and operation principle.

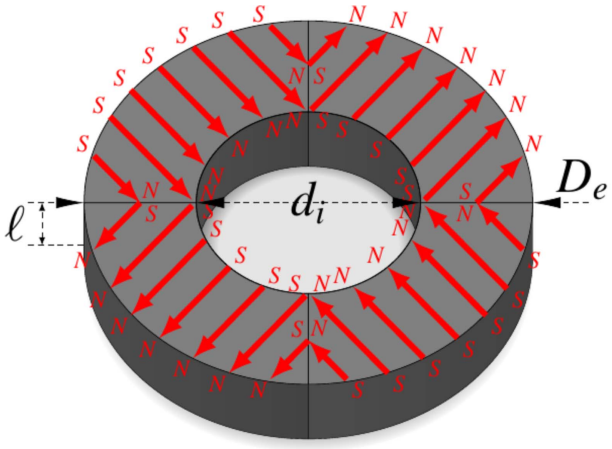

Physical Characteristics
$B_r = 1.36$ T;
$H_c = 10.2 \times 10^5$ A/m;
$T_{max} = 150$ °C;
Dimensions (mm)
$D_e = 55.8$ (± 0.05);
$d_i = 30$ (± 0.05);
$\ell = 13$ (± 0.05);

Figure 2. The permanent magnets system.

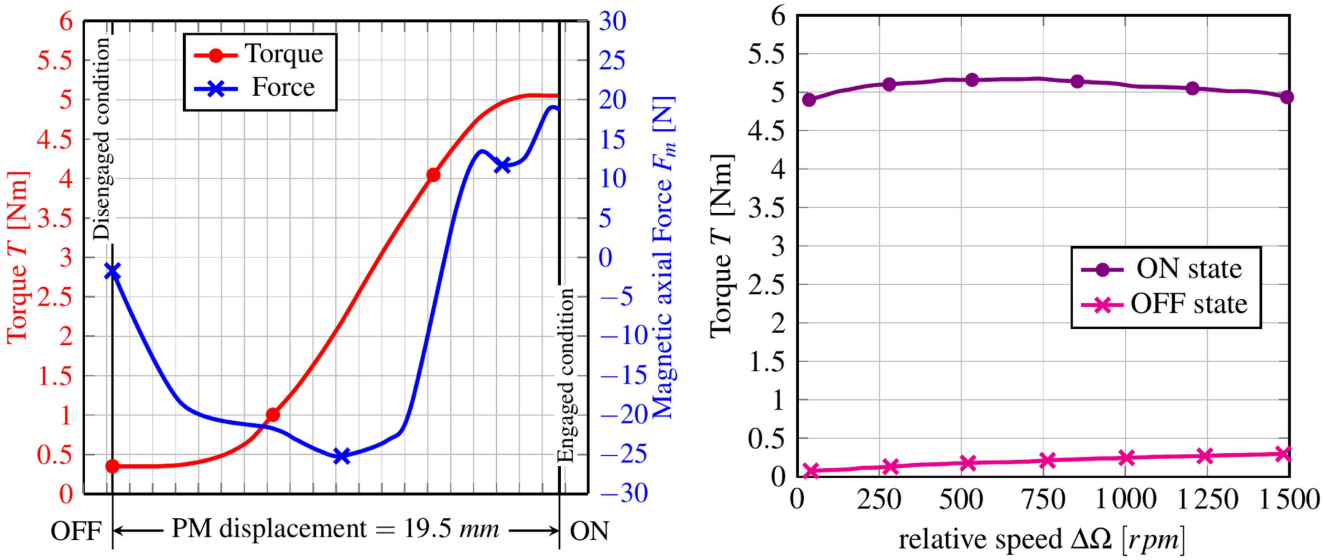

(a) Torque and axial force vs PMs displacement (b) Torque vs relative speed $\Delta\Omega$

Figure 3. Torque and magnetic axial force in the previously developed prototype.

(a) Schematic view (b) Real shaft

Figure 4. The primary shaft: 'old device'.

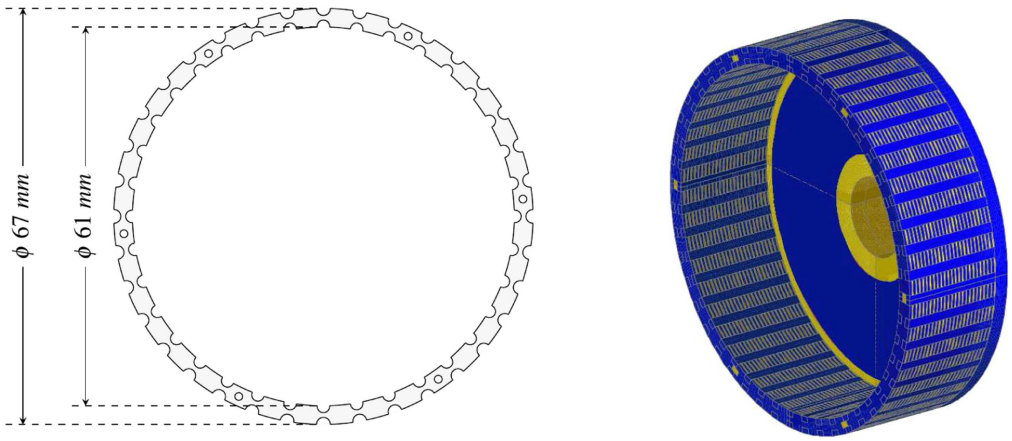

(a) Ferromagnetic layers (b) Schematic view

Figure 5. The primary shaft: new configuration.

and outer MRF gap, allowing a better field distribution inside the MR fluid itself.

However, in order to exploit electrodynamic effects, the primary shaft needs to be completely re-designed from an electro-magnetic point of view. The schematic view of the new solution is shown in figure 5.

It consists of a number of thin ferromagnetic layers (thickness 0.5mm), with 36 slots and teeth machined on the inner and outer diameter. Once stacked, the laminated core slots are filled with a conductive alloy of about $3 \times 10^7\ \Omega^{-1}\ \mathrm{m}^{-1}$, short-circuited around the ends by two rings. In this way a kind of double 'squirrel cage' can be obtained: one positioned at the outer radius of the inner gap, and the second at the inner radius of the outer gap. This new design has two effects: (1) the ferromagnetic layers (laminations) allows to better address the magnetic flux density in the two cylindrical portions of the MRF gap; (2) the double-cage permits the circulation of the eddy currents and an extra torque can be obtained.

Therefore, the device at the startup operates like an induction motor in which the rotating magnetic fields is obtained by the mechanical rotation of the four-pole PMs rotor. In fact, during the electro-mechanical transient phase, when the two clutch shafts rotate at different speeds, the permanent magnets induce eddy currents on the (double) squirrel cage. The interaction between the eddy currents and the magnetic induction produces an electromagnetic torque which, added to that of the MRF, helps the clutch engagement. When the relative speed between the clutch shafts is zero (engaged condition), the eddy currents, and consequently the electromagnetic torque, vanish and the torque transmission is assured by the MRF only. The proposed solution allows a smart increase of the clutch transmissible torque, especially during the starting phase when extra torque could be necessary to overcome possible static frictions.

4. Numerical simulations of the *new* device

The performance of the new device was investigated by developing a 3D dynamic model, based on the FEM code EFFE [11]. It is able to take into account the materials non-linearity (ferromagnetic iron and MR fluid), the permanent magnets behavior, as well as the motional effect due to the

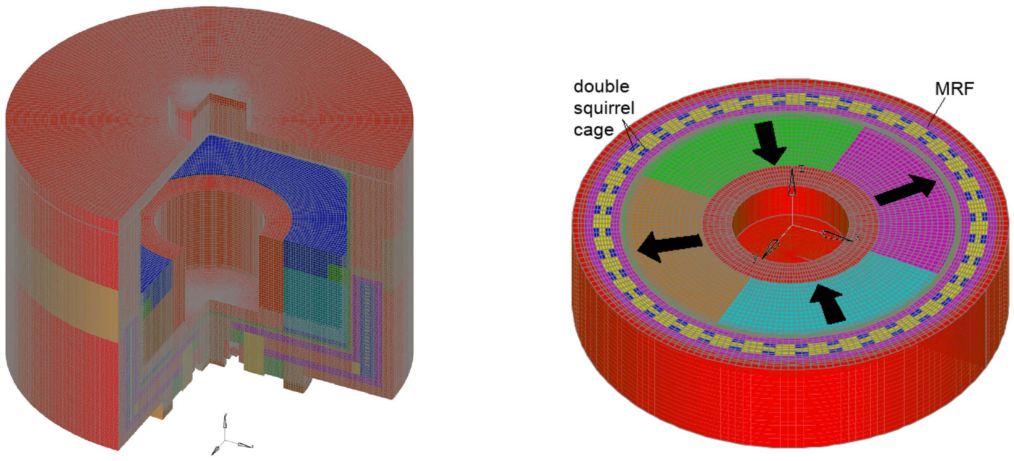

(a) Whole model (b) Particular of the double squirrel cage

Figure 6. 3D FE model of the device.

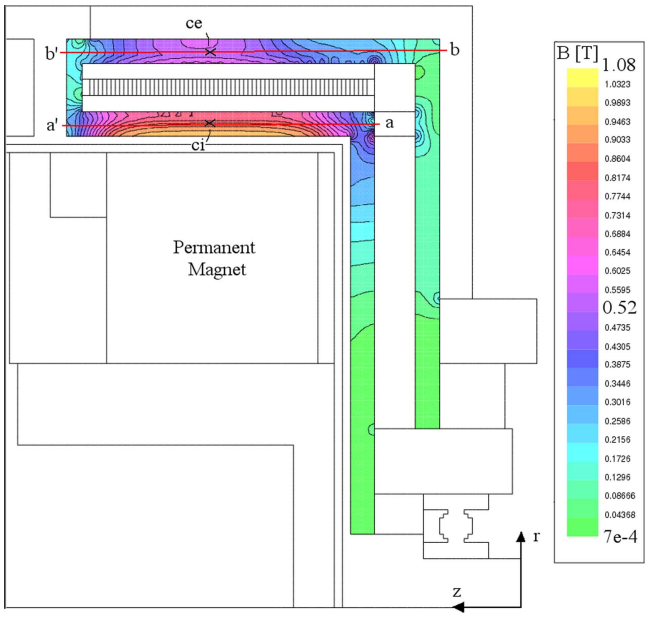

Figure 7. The map of B inside the MRF (new device).

PMs rotation around the device axis. Figure 6(a) shows the FE mesh of the whole structure, containing about 2.5×10^6 elements and nodes, while figure 6(b) show a cut in the FE model at the level of the double squirrel cage.

4.1. Static conditions

In order to analyze the behavior of the magnetic flux density inside the MR fluid, some numerical simulations were carried out with the clutch at rest (the primary and secondary shaft speed was fixed to zero) and with the PMs in the ON state. Figure 7 shows the map of the magnetic flux density B inside the fluid in the new device, while in figure 8 the comparison between the B field in different parts of the gap, for the new and 'old' device was reported. In particular, figures 8(a) and (b) respectively show the profile of the radial component of B along the lines $a - a'$ and $b - b'$ (as indicated in figure 7). Figures 8(c) and (d), instead, show the profile of the modulus of B along the circumferences passing respectively through the point *ce* and *ci* (see figure 7). Although the presence of of teeth and slots influences the profile of the magnetic flux density along the circumferential direction, the results show that the new configuration allows to slightly increase the values of B in the outer cylindrical part of the MRF.

4.2. Dynamic conditions

The new device was also investigated under dynamic conditions in order to evaluate the contribution of the double squirrel cage to the performance of the proposed device. The simulations were carried out imposing the smooth speed profile shown in figure 9 to the primary shaft, while keeping blocked the secondary one. As a consequence, the relative speed $\Delta\Omega$ between the primary and secondary shaft increased from 0 to 1500 rpm in about 120 ms. The analysis was performed in two different configurations: (1) the device without MRF in the gap; (2) the device with MRF in the gap.

4.2.1. Device without MRF in the gap: Although this condition does not refer to the real operation of the clutch, it could be useful to experimentally validate the FEM model. In fact, when the device does not contain the fluid, if the parasitic torque produced by the bearings friction is neglected, the clutch transmits only the (electromagnetic) torque due to the eddy currents. Figures 10(a) and (b) show the maps of the eddy currents in the double squirrel cage and the electromagnetic torque when the relative speed $\Delta\Omega$ follows the profile shown in figure 9, and the device does not contain the MRF. The steady state value of the electromagnetic torque is about 0.62 N m at $\Delta\Omega = 1500$ rpm.

4.2.2. Device with MRF in the gap: This condition refers to the real operation of the clutch. Since the MRF magnetic permeability is greater than that of the air, its presence in the

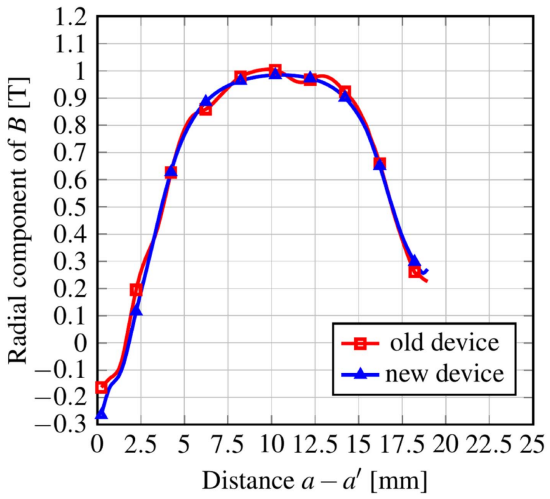

(a) B_r along the line $a-a'$

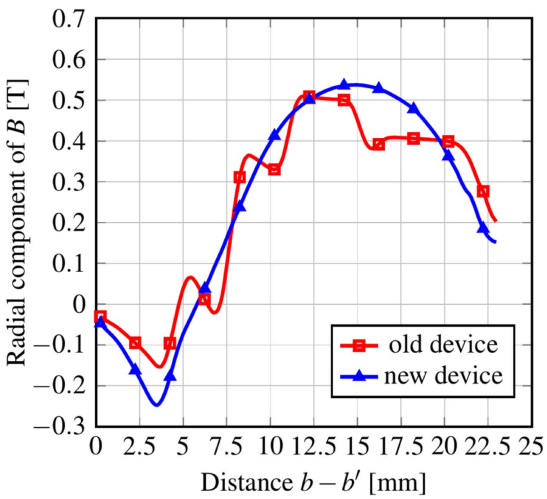

(b) B_r along the line $b-b'$

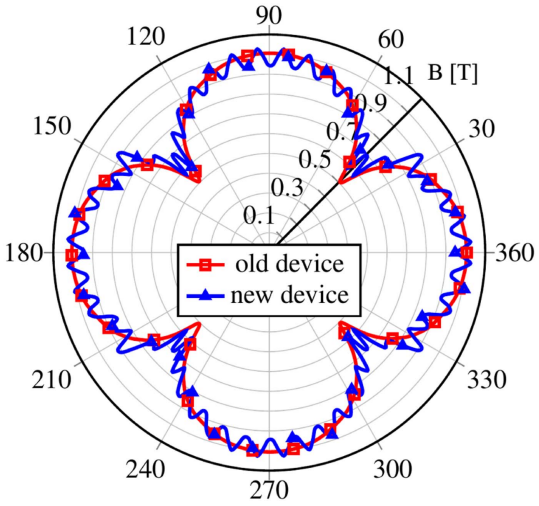

(c) $|B|$ along the circumference through ci

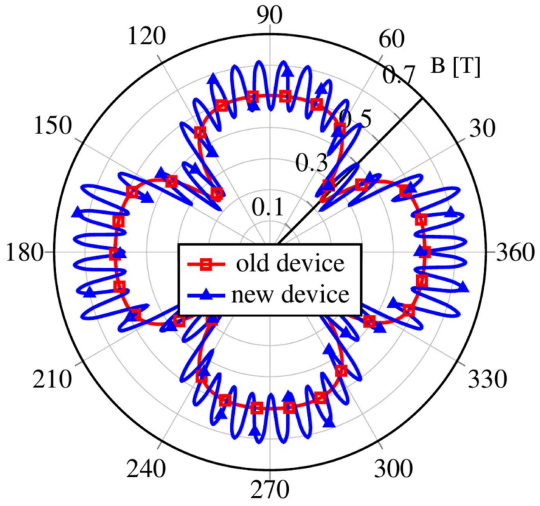

(d) $|B|$ along the circumference through ce

Figure 8. Comparison between the B field in different parts of the gap, for the new and 'old' device (see figure 7 for the lines and points where the field was simulated).

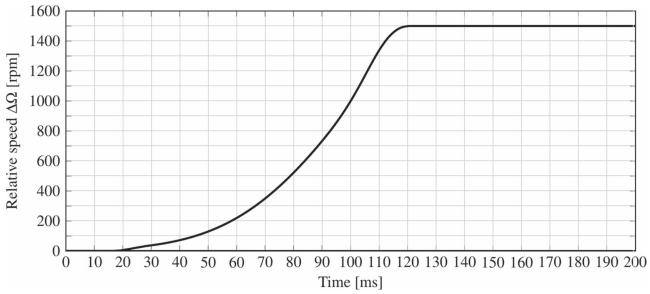

Figure 9. The profile of the (imposed) relative speed $\Delta\Omega$ between the primary and secondary shaft.

gap modifies the field lines, generally increasing the magnetic field in the whole structure. As a consequence, it is expected an increased electromagnetic torque with respect to the case without the fluid. Figures 11(a) and (b) show the maps of the eddy currents in the double squirrel cage and the electromagnetic torque in the same conditions of figure 10, but the gap filled with the MRF.

These numerical results show that the double squirrel cage solution operates correctly and it is capable to produce an effective electromagnetic torque. Furthermore, the presence of the fluid inside the gap allows to increase this torque, which at a speed of 1500 rpm is about 0.93 N m, that is about 50% bigger than the case without the fluid.

5. Experimental characterization of the clutch

On the basis of the results of numerical simulations, a prototype of the proposed electrodynamic/magnetorheological clutch was built. Figures 12(a)–(c) show respectively the ferromagnetic layers, the primary shaft with the double squirrel cage, and the assembled prototype.

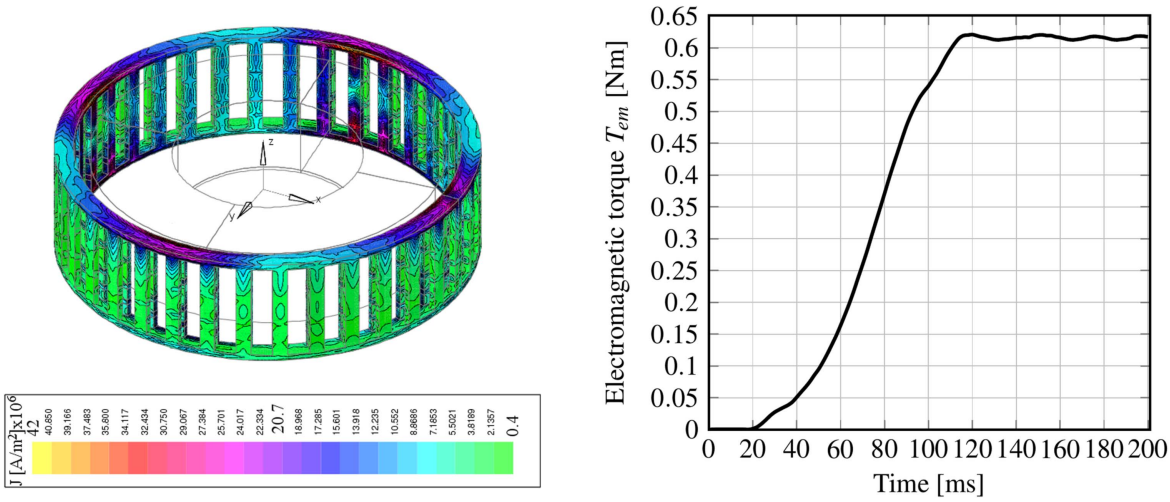

(a) The map of eddy currents in the double-cage (b) Electromagnetic torque

Figure 10. Map of the eddy currents and electromagnetic torque in the configuration without MRF in the gap.

In order to characterize its performance, the new prototype was tested on a dedicated test bench, as shown in figure 13. It was mainly composed of a brushless motor, coupled to the primary clutch shaft through suitable joints and ball bearings. The transmissible torque and the speed were measured by a torque meter (STAMOSENS 0160 DM).

As for the actuation system, although for the specific application a pneumatic actuator was recognized as the most suitable solution (see end of section 2, page 4), during the experimental tests described in the present paper, the clutch engagement/disengagement was obtained by using a different solution. In particular, the movement of the PM system from the OFF to the ON state (clutch engagement) was performed by using a preloaded spring, while the reverse movement (PM system from the ON to the OFF state: clutch disengagement) was assured by a stepper motor. As shown in the figure 13, this latter movement was obtained by using a wire fixed to the PM support and a pulley on which the wire can be wrapped. Then, the PM position inside the housing chamber was properly adjusted by controlling the stepper motor. This choice allows a fine control of the clutch actuation during the tests.

In all the experimental tests the primary shaft was properly driven by the brushless motor, while the secondary shaft was kept blocked by a mechanical constraint. The brushless motor was controlled by a dedicated software running on a PC and the measured quantities were recorded via USB.

As a first step, in order to verify the reliability of the dynamic FEM model, some preliminary experimental measurements on the new device in the configuration without the MRF were performed. The brushless motor was controlled in such a way that the primary shaft followed a given speed profile ('speed control' mode). Then, the PM excitation system was properly positioned along the axial direction in order to test the clutch in the disengaged condition (OFF state), in the engaged condition (ON state) or during the mechanical transient (from the OFF to the ON state). Furthermore, a comparison between the new and the old device operating in the same conditions was carried out. Figure 14(a) shows the speed and the torque measured in a test carried out with the clutch in the OFF state and without the MR fluid in the gap. Under this condition, the clutch transmits only the parasitic torque due to the bearings friction, which is approximately equal to 0.12 N m at 1500 rpm.

In figure 14(b) a preliminary validation of the dynamic FEM model is shown. In this test, with the clutch in the OFF state, the primary shaft was accelerated up to the speed of 1500 rpm. Then, at time $t \simeq 200$ s, the PM system was moved from the OFF to the ON state, performing the clutch engagement. Finally, at time $t \simeq 250$ s, the PM was brought back to the OFF state, and the clutch was slowed down until its stop. During the engaged condition (between time $t \simeq 200$ s and $t \simeq 250$ s), since the gap was empty, the torque meter measured a torque which is the sum of the parasitic and the electromagnetic torque. This latter is the torque due to the interaction between the eddy currents in the double squirrel cage and the excitation magnetic field. The average value of this torque is approximately equal to 0.67 N m at 1500 rpm. Therefore, subtracting the parasitic torque (see figure 14(a)), the average value of the experimental electromagnetic torque at 1500 rpm is about 0.56 N m. Taking into account that the simulation results reported in figure 10(b) neglect the parasitic torque, the error between the calculated electromagnetic torque and the measured one is about 10%, demonstrating that the developed FEM model is able to satisfactorily predict the dynamic behavior of the proposed device.

Figure 14(b) shows that also in the old device an electromagnetic torque exists. In fact, eddy currents are induced also in the materials which compose the old primary shaft (see figure 4). Anyhow, since the electrical conductivity of these materials is several times lower than that of the double-cage material, the contribution of the electromagnetic torque in the old device can be neglected.

A second set of measurements was performed on the prototype with the MR fluid in the gap and for different

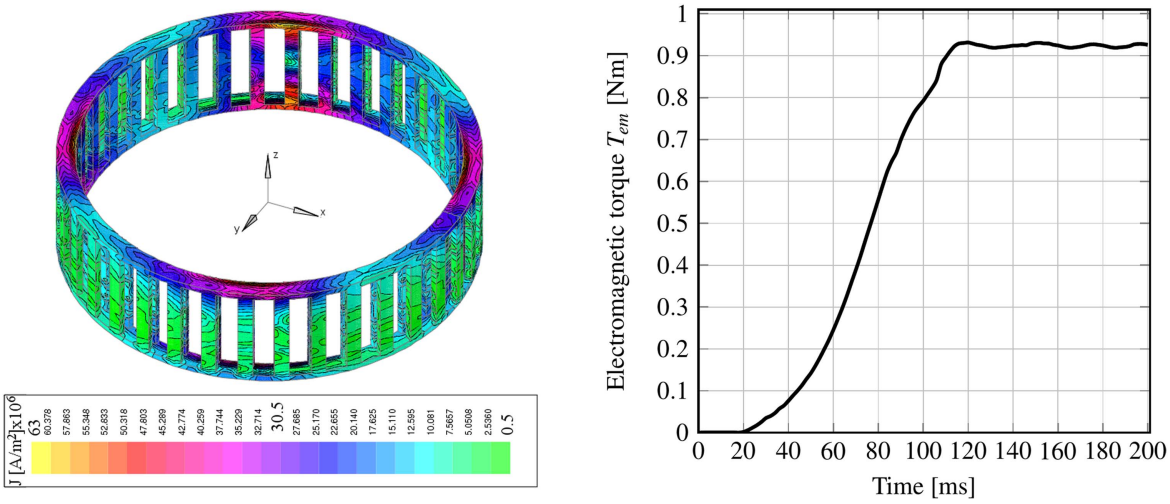

(a) The map of eddy currents in the double-cage (b) Electromagnetic torque

Figure 11. Map of the eddy currents and electromagnetic torque in the configuration with MRF in the gap.

(a) Ferromagnetic layers (b) Primary shaft with double squirrel cage (c) The final prototype

Figure 12. The clutch prototype.

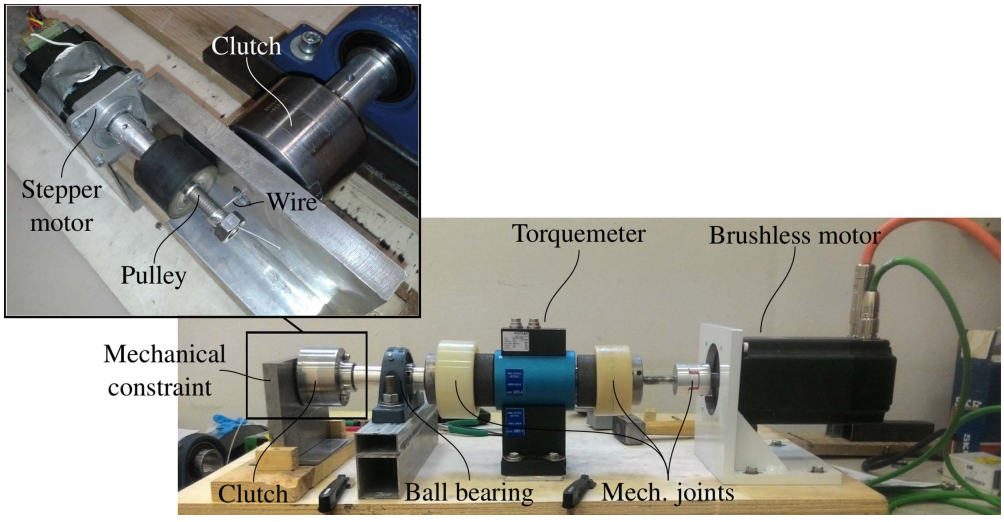

Figure 13. The test bench, with the actuation system.

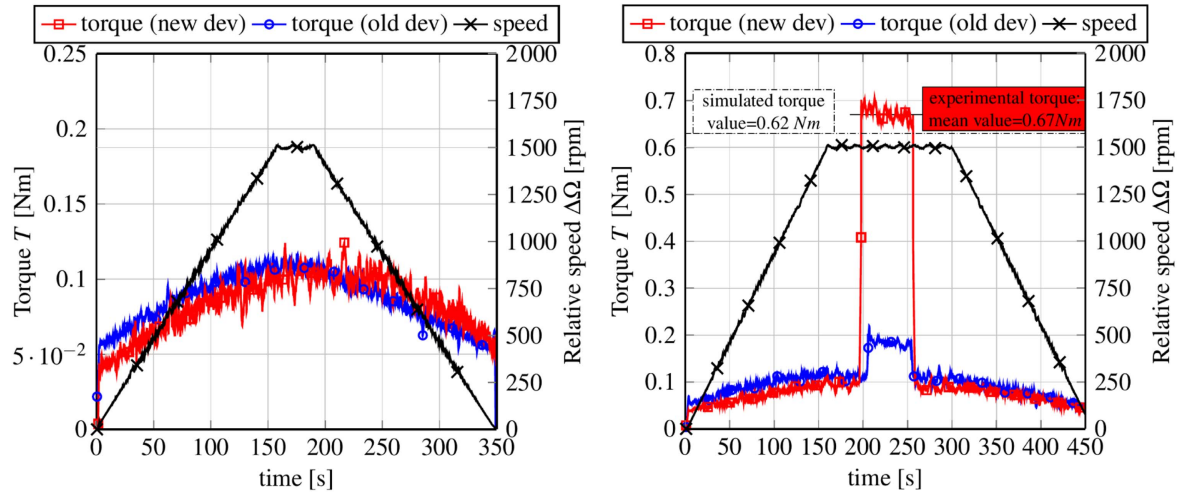

(a) OFF state: parasitic torque (b) Electromagnetic torque

Figure 14. Experimental tests without MRF in the gap.

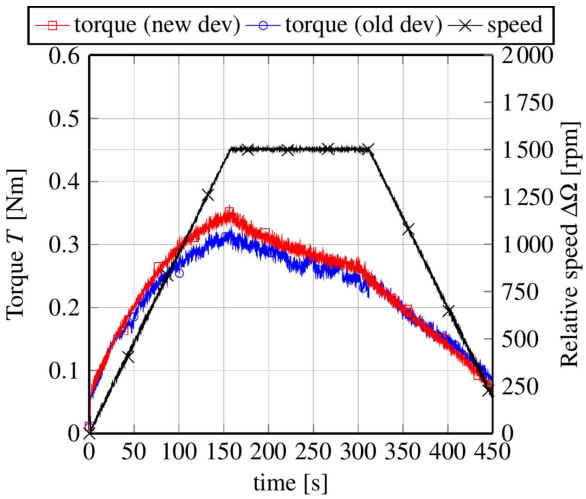

Figure 15. Experimental tests with MRF in the gap and PM in the OFF state: parasitic + viscous + residual field torque.

positions of the PM inside the housing chamber. Figure 15 shows the speed and the torque measured in a test carried out with the PM in the OFF state. Under this condition, besides the parasitic torque, the clutch transmits also the torque due to the viscosity and residual magnetization of the MR fluid. In fact, although the magnetic design of the device was performed trying to completely shield the MRF when the clutch is in the disengaged condition, a residual magnetic field passes through the fluid. With the PM system in the OFF state, the contribution of the torque due to the presence of the MRF can be approximately evaluated subtracting the parasitic torque (see figure 14(a)). The result indicates that the sum of the viscosity and residual field torque is approximately equal to 0.25 N m at 1500 rpm. Furthermore, the comparison between the new and the old device shows that the design of the new primary shaft has only a little influence on the performance of the clutch in the disengaged condition.

Moreover, in order to verify the effectiveness of the proposed solution, a test considering the mechanical transient of the clutch from the disengaged condition to the engaged one was carried out. The brushless motor accelerated the primary shaft from 0 to 1500 rpm in about 150 s, then the speed was kept constant by the control system. Since the secondary shaft was blocked, the relative speed between the two shafts was $\Delta\Omega = 1500$ rpm. Once the speed have reached its final value, at about $t = 181$ s the PM system was moved from the OFF to the ON state. Then, after about 6–7 s the brushless motor was turned off. In figure 16 the speed and the torque recorded during this test were shown. In the same figure, the comparison between the new and the old device was reported. The results show that the torque transmitted by the new device reaches a value of about 6.5 N m, that is about 25%–28% bigger than the torque obtained by means the old device (≃5.1 N m). As for the speed, since the brushless motor was driven in the 'speed control' mode, during the engagement phase a speed sag of about 11%–13% happened due to the increasing of the torque.

As a secondary matter, it is noteworthy that once the clutch is engaged, the profile of the torque decreases almost linearly with the time. This behavior can be explained considering the well known effects of temperature on the torque transmission characteristic of an MRF-based clutch [12–14]. In fact, since the relative speed between the two shafts increases the work dissipated inside the device, the self-produced heat increases the temperature of the fluid and a loss of torque can be experienced. Obviously, this effect is more prominent in the new clutch with respect to the old one, since the eddy currents induced in the double squirrel cage contribute to further increase the temperature of the MRF.

5.1. The real clutch operation

The experimental tests carried out in the previous section were performed controlling the brushless motor in a 'speed control' mode. Such kind of control allowed to impose a given profile of relative speed $\Delta\Omega$ between the primary and secondary clutch shaft and to measure the transmissible

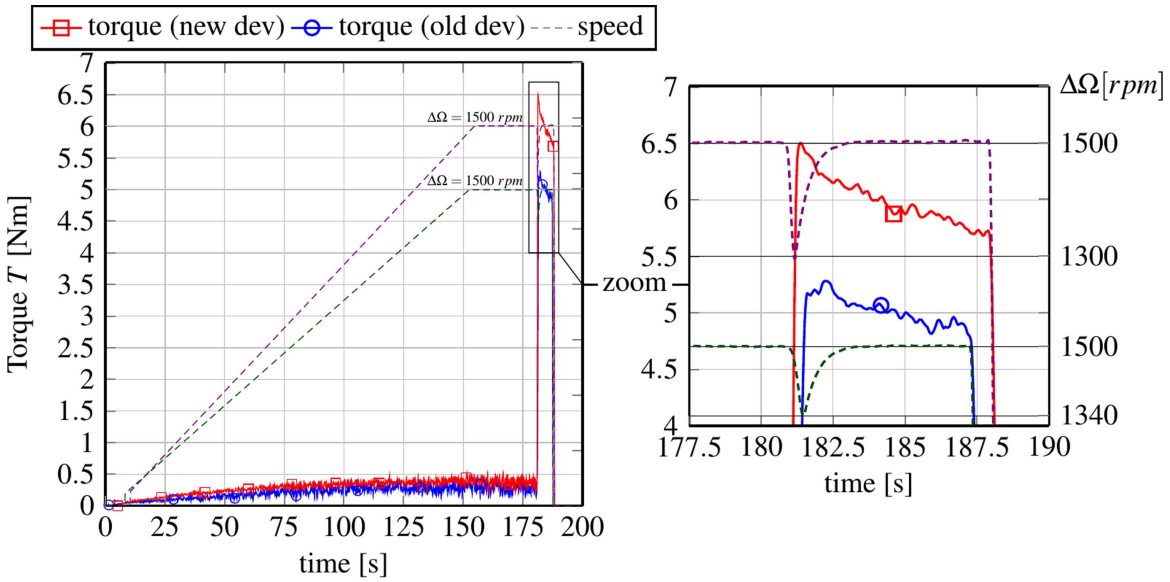

Figure 16. Experimental tests with MRF in the gap: PM from OFF to ON state under speed control.

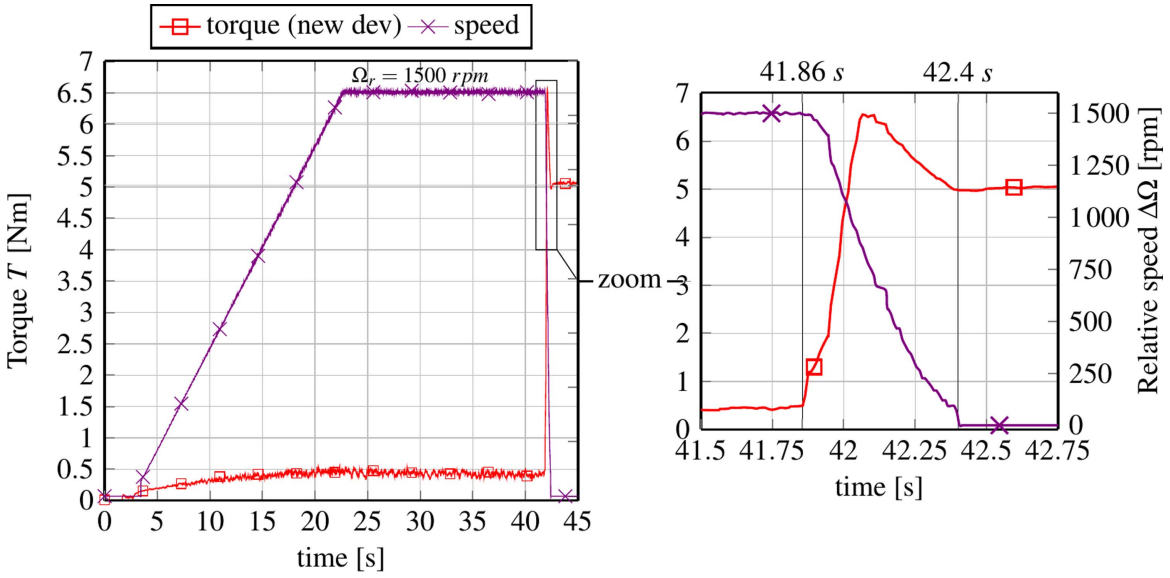

Figure 17. The real clutch operation. Experimental tests with MRF in the gap, PM from OFF to ON state under torque control.

torque for different positions of the PM inside the housing chamber. Although these tests were useful in analyzing the contribution of the eddy currents to the torque transmitted by the proposed device, they cannot reproduce the real operation of a clutch. As a matter of fact, in order to verify the real behavior of the device, the brushless motor was driven in a 'torque control' mode. This control considers two given reference values (thresholds): one for the speed (1500 rpm) and another for the torque (1 N m). If the torque transmitted by the clutch is below the prefixed threshold, the brushless motor accelerates the primary shaft with a given ramp, reaching the speed reference value. On the contrary, if the transmitted torque exceeds the given threshold, the brushless motor adjusts its speed in accordance with the value of the torque, operating like a mechanical load.

The profiles of the torque and of the (relative) angular speed measured by the torque meter in this experimental test are shown in figure 17.

In the first phase of the test (from $t \simeq 0$ s to $t \simeq 41.86$ s), the clutch was in the disengaged condition and the primary shaft was accelerated from 0 to 1500 rpm. Since the PM system was in the OFF state, the MR fluid was not excited, the eddy currents were negligible and the parasitic+viscous +residual field torque ($\simeq$0.5 N m) was not able to actuate the secondary shaft. Under these conditions, the primary shaft was accelerated until it reaches and maintains the speed value equal to the prefixed threshold (1500 rpm).

At the time $t \simeq 41.86$ s, the preloaded spring pushed the PM in the ON state, performing the clutch engagement. During the electro-mechanical transient (from $t \simeq 41.86$ s to

$t \simeq 42.4$ s), the transmitted torque increased as a function of the PM displacement along the z-axis, while the relative speed accordingly decreased. In this case, the instrumentation measured a total torque of about 6.6 N m, which mainly is the sum of two components; the first one is due to the magnetization of the MR fluid and follows the profile shows in figure 3(a). The second component, related to the electrodynamic effects, is produced by the interaction between the eddy currents in the double squirrel cage and the magnetic field. This electromagnetic torque exists only during the mechanical transient when the relative speed between the two clutch shafts is non-zero ($\Delta\Omega \neq 0$). It acts in the device as an extra torque which is added to the torque obtained by the excitation of the MR fluid, helping the clutch engagement when possible static frictions have to be overcome. However, once the system reaches its mechanical equilibrium, since the slip becomes zero ($\Delta\Omega = 0$), the eddy currents vanish and the torque transmission is assured only by the MRF, as in a conventional MR-based clutch.

Finally, the results show that the total torque during the mechanical transient was increased by about 28% as compared with the clutch without the double squirrel cage.

As for the heat problem, although it requires a more in-depth analysis, it could be observed that during the real operation of the clutch, the contribution of the eddy currents to the temperature rising occurs only during the mechanical transient, which is of very short duration (about 0.5 s).

6. Conclusions

The magnetic design and experimental characterization of an innovative multi-gap clutch based on MRFs and electrodynamic effects were presented in this paper. It was based on a magnetorheological clutch excited by permanent magnets, and exploits the electrodynamic effects to improve its performance of about 28%. During the engagement (transient) phase, the rotation of the PM-based excitation system induces 'eddy currents' on a double squirrel cage, strategically positioned in the device. Then, the interaction between these currents and the magnetic field produces an electromagnetic torque. This torque is added to the one transmitted by the magnetized MR fluid, helping the clutch engagement, especially during the starting phase when an extra torque could be necessary to overcome possible static frictions. Once the two shafts reach the same speed, the eddy currents (and consequently the electromagnetic torque) vanish and the torque transmission is assured by the MRF only, as in conventional MRF-based clutch. The proposed clutch was designed by means a 3D dynamic FEM model and the performance under different operating conditions was verified by experimental measurements on a prototype.

Acknowledgments

This work was funded by Pierburg Pump Technology Italy, S. p.A., within a framework of a project supported by Regione Toscana, P.O.R., C.R.e.O., F.E.S.R. 2007-2013.

References

[1] Rizzo R, Musolino A, Bucchi F, Forte P and Frendo F 2015 A multi-gap magnetorheological clutch with permanent magnet *Smart Mater. Struct.* **24** 075012
[2] Bucchi F, Forte P and Frendo F 2014 A fail-safe magnetorheological clutch excited by permanent magnets for the disengagement of automotive auxiliaries *J. Intell. Mater. Syst. Struct.* **25** 2102–14
[3] Armenio G, Bartalesi E, Bucchi F, Ferri A, Frendo F, Forte P, Rizzo R and Squarcini R 2011 Mechanical combustion engine driven fluid pump *EPO Patent* 11425176.2-2423
[4] Shiao Y and Nguyen Q 2013 Development of a multi-pole magnetorheological brake *Smart Mater. Struct.* **22** 065008
[5] Guo H T and Liao W H 2012 A novel multifunctional rotary actuator with magnetorheological fluid *Smart Mater. Struct.* **21** 065012
[6] Bucchi F, Forte P, Frendo F and Squarcini R 2013 A magnetorheological clutch for efficient automotive auxiliary device actuation *Frattura Integritá Strutturale* **7** 62–74
[7] Wu J, Jiang X, Yao J, Li H and Li Z 2016 Design and modeling of a multi-pole and dual-gap magnetorheological brake with individual currents *Adv. Mech. Eng.* **8** 1–15
[8] Bucchi F, Forte P and Frendo F 2015 Analysis of the torque characteristic of a magnetorheological clutch using neural networks *J. Intell. Mater. Syst. Struct.* **26** 680–9
[9] L. C. Ltd., www.lord.com/products-and-solutions/magneto-rheological-(mr)/mrproducts.xml
[10] Bartalesi E, Bucchi F and Squarcini R 2014 Vacuum actuation for axial movement of a magnet in a magnetorheological clutch *EPO Patent* WO2012EP66463 20120823
[11] EFFE, EFFE v2.00 user manual, Bathwick Electrical Design ltd, 2009
[12] Zschunke F, Rivas R and Brunn P O 2005 Temperature behavior of magnetorheological fluids *Appl. Rheol.* **15** 116–21
[13] Bucchi F, Forte P and Frendo F 2015 Temperature effect on the torque characteristic of a magnetorheological clutch *Mech. Adv. Mater. Struct.* **22** 150–8
[14] Yildirim G and Genc S 2013 Experimental study on heat transfer of the magnetorheological fluids *Smart Mater. Struct.* **22** 085001